Scientific paper

Kinetics of Crystal Violet Fading in the Presence of TX-100, DTAB and SDS

Babak Samiey* and Fatemeh Ashoori

Department of Chemistry, Faculty of Science, University of Lorestan, 68137-17133, Khoramabad, IRAN

** Corresponding author: E-mail: babsamiey@yahoo.com*

Received: 24-07-2010

Abstract

The rate constant of alkaline fading of crystal violet (CV^+) was measured in the presence of non ionic (TX-100), cationic (DTAB) and anionic (SDS) surfactants. This reaction was studied at 283–303 K. The rate of reaction showed remarkable dependence on the electrical charge of the used surfactants. It was observed that the reaction rate constant increased in the presence of TX-100 and DTAB and decreased in the presence of SDS. Binding constants of CV^+ with TX-100 and DTAB and the related thermodynamic parameters were obtained by classical (or stoichiometric) model. The results show that binding of CV^+ to TX-100 is endothermic and binding of CV^+ to DTAB and SDS is exothermic in the used concentration range of surfactants.

Keywords: Classical model, crystal violet, kinetics, fading, surfactant

1. Introduction

The rates of chemical reactions are known to be changed by self-organized assemblies such as micelles.[1–9] Effects of micelles on these reactions can be attributed to electrostatic and hydrophobic interactions. Crystal violet (CV^+) is a triphenylmethane dye.[10] This dye is used as biological stains, in verterinary medicine and as a dye for silk, wood, cosmetics, and food.[11] Surfactants can affect on the kinetics of the alkaline fading of dyes and other compounds and were studied by many researchers.[12–19] In continuation of our earlier works,[20–22] we studied the CV^+ alkaline fading in the presence of different concentrations of TX-100 (nonionic), DTAB (cationic) at 283–303 K and in the presence of SDS (anionic) at 323 and 333 K. The CV^+ fading is a one-step reaction and kinetics of these kinds of reactions in the presence of surfactants can be studied using pseudo-phase ion exchange, cooperativity and classical (or stoichiometric) models.[20–22] Also, in this work, effects of substituent groups of CV^+, malachite green (MG^+), brilliant green (BG^+) and electric charge of bromophenol blue ($BPB^=$) on the fading reaction rates of these triphenylmethane dyes were compared to each other.

2. Experimental

2. 1. Materials and Methods

Crystal violet, polyoxyethylene (number of segments 9.5) glycol *tert*-octylphenyl ether (Triton X-100 or TX-100), dodecltrimethylammonium bromide (DTAB), sodium dodecyl sulfate (SDS) and NaOH were purchased from Merck.

The fading of CV^+ was followed at its maximum wavelength (λ_{max}) values in a thermostated cell compartment of a Shimadzu UV–1650PC spectrophotometer. The reaction of CV^+ with hydroxide ion brings about fading the color of the CV^+ and results in the formation of colorless carbinol base, Fig. 1. The experiments were conducted at 283–333 K within ± 0.1 K. All the kinetic runs were carried out at least in triplicate. In the case of TX-100 and DTAB, to perform each kinetic run, a 100 *μl* aliquot of 2×10^{-4} M CV^+ solution was added by a microsyringe into 3 ml of a solution containing 4.42×10^{-3} M sodium hydroxide and a certain concentration of surfactant. To study all interactions occurred between surfactant and substrate molecules, we carried out the experiments in the surfactant concentration range which reaction rate finally reaches to its maximum value (in the case of catalytic ef-

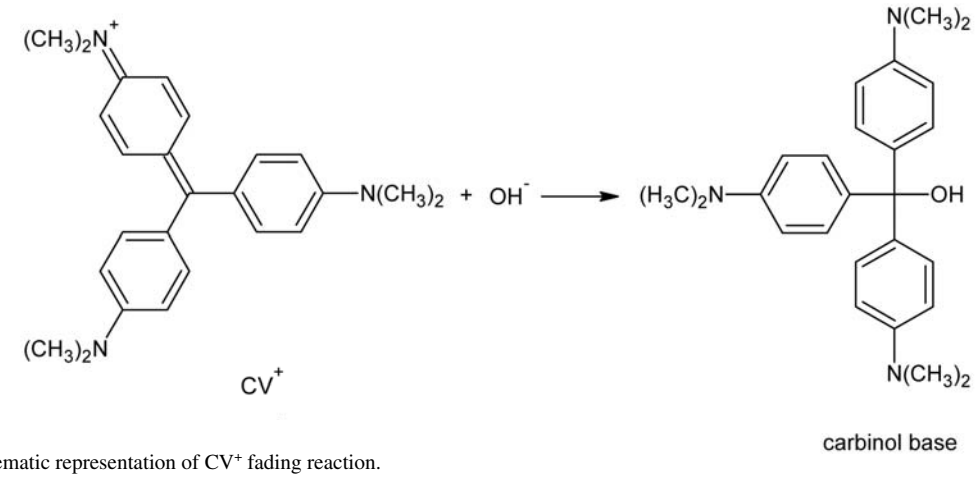

Figure 1. Schematic representation of CV^+ fading reaction.

fect) or becomes very slow (in the case of inhibitory effect). The reaction between CV^+ and hydroxide has been found to be bimolecular but pseudo-first-order conditions (excess alkali) were used in all cases. We used the second-order reaction rate constants in our calculations.

3. Results and Discussion

3. 1. Analysis of Kinetic Data by Classical Model

In classical (or stoichiometric) model[21] it is assumed that in each range of surfactant concentration, the surfactant and substrate can bind together and there is an equilibrium relation between them. A concentration of surfactant is called "*substrate-surfactant complex formation point*" (or abbreviated as *sc* point) in which the equilibrium relation between added surfactant and species already presented in solution ends and a new equilibrium relation between added surfactant and compound resulted from the previous equilibrium relation starts. Critical micelle concentration (*cmc*) value of a surfactant is also a *sc* point and there may be some *sc* points before and after *cmc* as well. The range of surfactant concentration which covers an equilibrium relation is named "*region*". Surfactant molecules can bind to the substrate either monomeric or micellar (by one or more number of their molecules). Thus, we can obtain the stoichiometric ratios and binding constants of interactions of surfactants with substrate molecules in various ranges of surfactant concentrations. For each assumed equilibrium relation, following equation holds for:

$$\ln k' = c - \frac{E_S}{RT}[S]_t \qquad (1)$$

where k', c, $[S]_t$, R and T are the rate constant in the presence of surfactant, ln$k$ (at first region) or ln k_{sc} (for other regions), total surfactant concentration, universal gas constant, absolute temperature, respectively. E_S is the catalytic or inhibition energy of reaction in constant temperature and various surfactant concentrations. k_{sc} is the k_{obs} in the starting of every region except region one. Equation (1) is introduced as "Samiey equation"[21] and can determine the concentration range of each region.[21] If the reaction rate is decreased upon increasing the surfactant concentration, the sign of E_S is positive and is called "*inhibition energy*" and if the reaction rate is increased with increasing the surfactant concentration, the sign of E_S is negative and is named "*catalytic energy*" at constant temperature and various surfactant concentrations. Dimension of E_s is in kJ (mol molar(surfactant))$^{-1}$.

In this model, it is assumed that in each region one substrate molecule, CV^+ in this work, binds to n molecules of surfactant and we have:

$$CV^+ + nS \overset{K}{\longleftrightarrow} S_nCV^+ \qquad (2)$$

where K is the binding constant of the substrate-surfactant interaction in each region. According to classical model[21] these interactions are of type I or II which surfactant has an inhibitory or catalytic effect on the fading reaction of CV^+, respectively and k_{obs} is related to the surfactant concentration as follows:[21]

$$k_{obs} = \frac{k + k_S K[S]_t^n}{1 + K[S]_t^n} \quad \text{(region one)} \qquad (3)$$

$$k_{obs} = \frac{k_{sc} + k_S K([S]_t - [sc])^n}{1 + K([S]_t - [sc])^n} \quad \text{(all the other regions)} \qquad (4)$$

where k and k_{sc} are the reaction rate in the absence of surfactant and at every *sc* point, respectively. k_s is the reaction rate in substrate-surfactant complex and where inhibition, $k_s = 0$. The total binding constant (K^i_{tot}) and total stoichiometric ratio (n^i_{tot}) values for each substrate, in the ith region, can be obtained from below equations:

$$K_{tot}^{i} = K_1 ... K_{i-1} K_i = \prod_{j=1}^{i} K_j \quad (5)$$

$$n_{tot}^{i} = n_1 ... n_{i-1} n_i = \sum_{j=1}^{i} n_j \quad (6)$$

Going from one region to the next one, if $K^{1/n}$value (the average binding constant of interaction between one substrate molecule with one surfactant molecule in each region) increases, the cooperativity of interaction is positive and if $K^{1/n}$value decreases, the cooperativity is negative.

3. 2. Effect of TX-100 on the CV^+ Fading

As seen in Fig. 2 and Table 1, kinetics of CV^+ fading in the presence of TX-100 is three-region at 283, 293 and 303 K. The *cmc* value of TX-100 in pure water is 0.29 mM.[24] The first *sc* point is above *cmc* of TX-100, Table 1. In the first region, increase in TX-100 concentration results in the red shift in λ_{max} value of CV^+, Fig. 3, but as seen in Fig. 2 and Table 1, the fading rate constant keeps approximately constant.

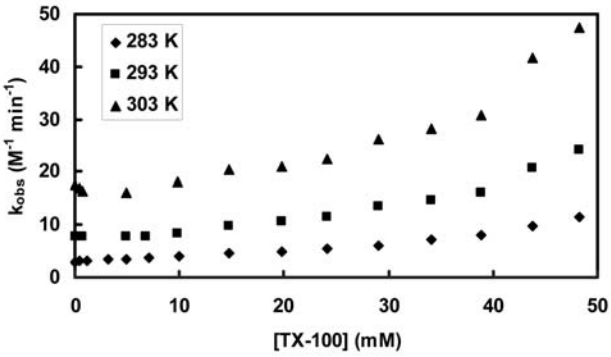

Figure 2. k_{obs} values of CV^+ fading reaction *vs.* concentrations of TX-100 under alkaline conditions.

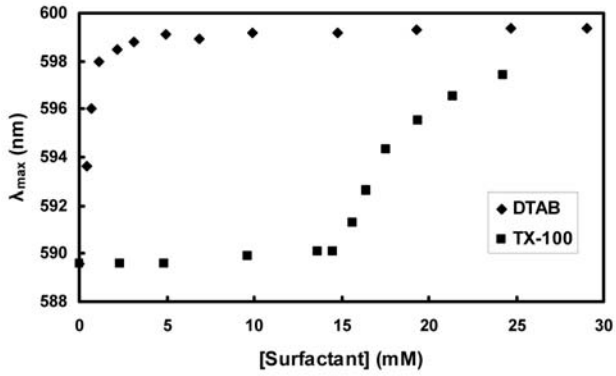

Figure 3. λ_{max} values of CV^+ *vs.* concentrations of DTAB and TX-100 under alkaline conditions.

Table 1. Parameters Obtained from Classical Model for Interaction of CV^+ with TX-100 at 283–303 K.

T (K)	Region	*sc* (mM)	k_{sc} ($M^{-1}min^{-1}$)	Samiey equation	E_s	*logK*	*n*	k_s ($M^{-1}min^{-1}$)	Cooperativity
283	**1st**	**0.00**	**2.95**	**Reaction rate is approximately constant**		**–**	**–**	**–**	↓+
	2nd	14.79	4.47	$\ln k' = 24.83[TX]_t + 1.11$	–58.8	1.71	1.57	32.70	↓+
	3rd	38.84	8.05	$\ln k' = 39.13[TX]_t + 0.57$	–92.1	5.09	2.31	13.04	
293	**1st**	**0.00**	**7.76**	**Reaction rate is approximately constant**		**–**	**–**	**–**	↓+
	2nd	19.75	10.65	$\ln k' = 21.87[TX]_t + 1.94$	–53.3	2.19	1.44	26.64	↓+
	3rd	38.84	16.10	$\ln k' = 43.37[TX]_t + 1.11$	–105.7	4.31	1.93	27.32	
303	**1st**	**0.00**	**17.64**	**Reaction rate is approximately constant**		**–**	**–**	**–**	↓+
	2nd	14.79	20.54	$\ln k' = 17.73[TX]_t + 2.73$	–44.7	3.56	2.27	44.14	↓+
	3rd	38.84	30.79	$\ln k' = 46.26[TX]_t + 1.66$	–116.5	4.22	1.82	52.38	

Dimension of E_s is in kJ (mol molar(surfactant))$^{-1}$. TX is an abbreviation for TX-100 and dimension of its concentration in Samiey equation is in M. Dimension of *K* is in M^{-n}.

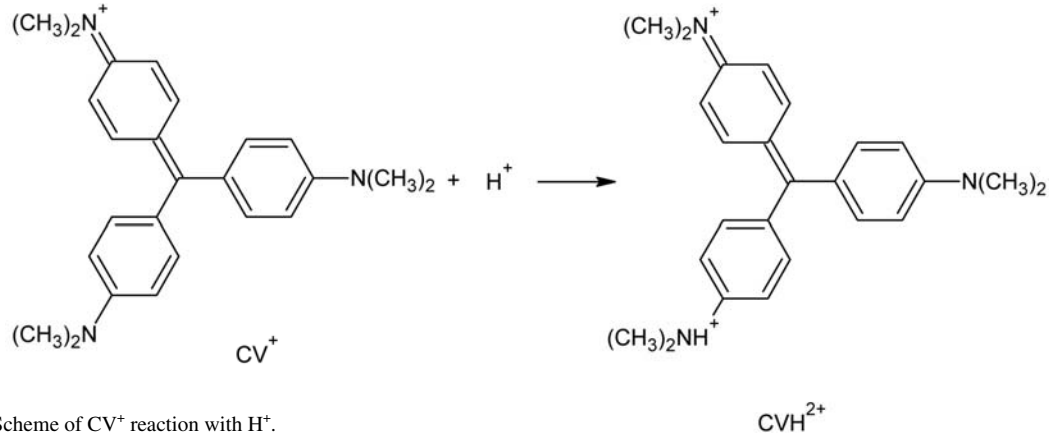

Figure 4. Scheme of CV^+ reaction with H^+.

The red shift has been previously reported for other compounds upon going from polar to apolar solvents.[21,25–27] This indicates that in this region, a preliminary weak electrostatic interaction occurs between $(CH_3)_2N^+$ = group of CV^+ and oxygen atom of ethoxy chains of TX-100 molecules which is similar to interaction of silanol groups of silica gel with TX-100.[24,28] This interaction along with further hydrophobic interaction of CV^+ with TX-100 molecules decreases dielectric constant of the CV^+ microenvironment. To confirm this result, in acidic solution, interaction of TX-100 with CVH^{2+} results in the red shift in λ_{max} value of CVH^{2+}, Table 2 and Fig. 4.

Table 2. Typical λ_{max} Values of CV^+ in the Presence of TX-100, DTAB and SDS in Acidic and Alkaline Solutions.

In 1M HCl	λ_{max} (nm)	In 4.28×10^{-3} M NaOH	λ_{max} (nm)
–	431.6, 630.6	–	591.0
1.13 mM TX-100	431.2, 631.4	1.13 mM TX-100	598.0
16.50 mM DTAB	431.0, 630.0	16.50 mM DTAB	592.6
0.10 mM SDS	430.8, 630.2	0.10 mM SDS	590.5
0.20 mM SDS	430.4, 629.8	0.20 mM SDS	590.5
0.40 mM SDS	428.4, 635.6	0.60 mM SDS	589.5
0.60 mM SDS	427.7, 635.8	0.80 mM SDS	589.5 551.5
1.00 mM SDS	426.6, 636.2	1.00 mM SDS	589.0 551.5

But, interaction of TX-100 with CV^+ in the first region is weak and can not result in a remarkable effect on the fading rate constant. In the second and third regions at 283, 293 and 303 K, λ_{max} value of CV^+ is approximately constant, Fig. 3, but the fading rate constant increases with increase in TX-100 concentration, Fig. 2 and Table 1. It seems that in the second and third regions, TX-100 molecules interact with TX-100 molecules bound to CV^+ in the first region. According to Hughs-Ingold rules for nucleophilic substitution reactions,[29,30] formation of the neutral carbinol base from two oppositely charged reactants is favorable in lower dielectric constant media (Table S1 in the supporting information).

Thus, in the second and third regions, the reaction rate constant increases with increase in TX-100 concentration, Fig. 2. As seen in Table 3, interaction of CV^+ with TX-100 molecules throughout concentration range of TX-100 is endothermic and its ΔS value is positive.

As seen in Fig. 5, $\Delta S^{\neq}$ and $\Delta H^{\neq}$ values of the CV^+ fading reaction in TX-100 are negative and positive, respectively. In each region, there is a linear relation between $\Delta S^{\neq}$ and $\Delta H^{\neq}$ values which indicates that in each *sc* point mechanism of reaction change due to interaction of different number of TX-100 molecules with CV^+ (Table S2 in the supporting information). [31,32]

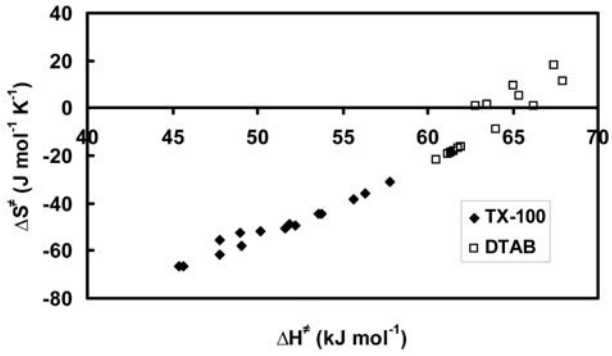

Figure 5. $\Delta S^{\neq}$ *vs.* $\Delta H^{\neq}$ values of CV^+ fading reaction in the presence of TX-100 and DTAB.

Table 3. Thermodynamic Parameters Obtained from Classical Model for Interaction of CV^+ with TX-100 at 283–303 K.

T(K)	*logK*	ΔG	ΔH	ΔS
		(kJ mol^{-1})		(J mol^{-1} K^{-1})
Region 2				
283	1.71	–9.3		
293	2.19	–12.3	150.6	562.1
303	3.56	–20.0		
Region 3				
283	5.09	–27.6		
293	4.31	–24.2	–72.2	–159.7
303	4.22	–24.5		
Regions 2 and 3				
283	6.80	–36.8		
293	6.49	–36.4	78.4	402.4
303	7.77	–45.1		

The total $\Delta H$and ΔS values were obtained from addition of the related values of the second and third regions. Dimension of K is in M^{-n}.

3. 3. Effect of DTAB on the CV+ Fading

As seen in Fig. 6 and Table 4, kinetics of CV^+ fading in the presence of DTAB is three-region.

The *cmc* value of DTAB in pure water is 13.77 mM[33] and the first *sc* point is approximately *cmc* of DTAB, Table 4. In the first region, with increase in DTAB concentration, the rate constant of CV^+ fading and λ_{max} value of CV^+ molecules keep approximately constant, Fig. 3 and Table 4. It seems that there is no interaction between CV^+ and DTAB molecules. Obviously, at the beginning of the second region (≈ 13.62 mM ≈ *cmc* value of DTAB), a weak electrostatic interaction occurs between $(CH_3)_2N$– group of CV^+ and positive head group of DTAB molecules and along with hydrophobic interaction of CV^+ with nonpolar moiety of DTAB molecules results in the red

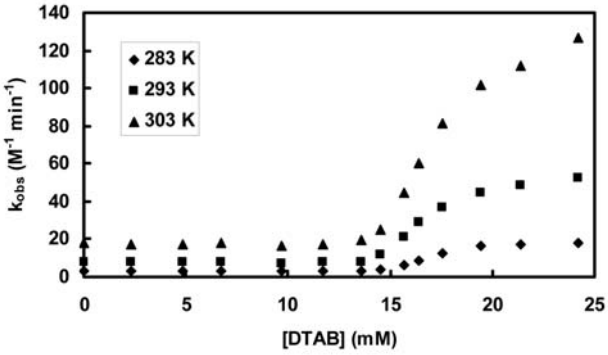

Figure 6. k_{obs} values of CV^+ fading reaction *vs.* concentrations of DTAB under alkaline conditions.

DTAB is exothermic and its ΔS value is negative. As seen in Fig. 5, $\Delta H^{\neq}$ values of the CV^+ fading reaction in DTAB are positive. In each region, there is a linear relation between $\Delta S^{\neq}$ and $\Delta H^{\neq}$ values which indicates that in *sc* points mechanism of reaction changes due to interaction of different number of DTAB molecules with CV^+(Table S3 in the supporting information).[31,32]

3. 4. Effect of SDS on the CV+ Fading

In aqueous solution CV^+ exhibits a maximum absorption band at 591 nm and a shoulder at about 553 and with increasing sodium dodecylsulfate concentration a new band at about 535 nm appeared, Fig. 7.

Table 4. Parameters Obtained from Classical model for Interaction of CV^+ with DTAB at 283–303 K.

T (K)	Region	*sc* (mM)	k_{sc} ($M^{-1}min^{-1}$)	Samiey equation	E_s	*logK*	*n*	k_s (M^{-1} min^{-1})	Cooperativity
283	**1st**	**0.00**	**2.95**	**Reaction rate is approximately constant**		**–**	**–**	**–**	↓+
	2nd	13.62	2.98	ln *k*' = 389.11[DTAB]$_t$ –4.26	–915.5	5.25	2.26	28.23	↓+
	3rd	19.43	16.29	ln *k*' = 19.75[DTAB]$_t$ –2.41	–46.5	4.47	1.84	18.91	
293	**1st**	**0.00**	**7.74**	**Reaction rate is approximately constant**		**–**	**–**	**–**	↓+
	2nd	13.62	8.21	ln *k*' = 397.80[DTAB]$_t$ –3.27	–969.0	4.61	1.91	63.91	↓+
	3rd	19.43	44.61	ln *k*' = 32.77[DTAB]$_t$ +3.17	–79.8	4.21	1.66	55.69	
303	**1st**	**0.00**	**17.64**	**Reaction rate is approximately constant**		**–**	**–**	**–**	↓+
	2nd	13.62	19.22	ln *k*' = 383.87[DTAB]$_t$ –2.27	–966.5	4.47	1.93	174.54	↓+
	3rd	19.43	101.52	ln *k*' = 46.17[DTAB]$_t$ +3.73	–116.3	4.06	1.69	144.86	

Dimension of E_s is in kJ (mol molar(surfactant))$^{-1}$. Dimension of DTAB concentration in Samiey equation is in M. Dimension of *K* is in M^{-n}.

shift in λ_{max} value of CV^+ molecules. Confirming this result, it is seen from Table 2 that 16.5 mM DTAB acidic solution has no effect on the λ_{max}value of CVH^{2+}. According to Hughs-Ingold rules for nucleophilic substitution reactions, under alkaline conditions, rate constant of CV^+ fading increases with increase in DTAB concentration.

Table 5. Thermodynamic Parameters of Interaction of CV^+ with DTAB Obtained from Classical Model at 283–303 K.

T(K)	$logK_{tot}$	ΔG (kJ mol^{-1})	ΔH	ΔS (J mol^{-1} K^{-1})
283	9.72	–52.6		
293	8.82	–49.5	–97.1	–158.9
303	8.54	–49.5		

Dimension of K_{tot} is in $M^{-n_{tot}}$.

In the third region, , the rate constant of CV^+ fading and λ_{max} value of CV^+ increase with increase in DTAB concentration. It shows that there is an interaction between CV^+ and DTAB molecules in its micelles, Fig. 6 and Table 4. As given in Table 5, interaction of CV^+ with DTAB molecules throughout concentration range of

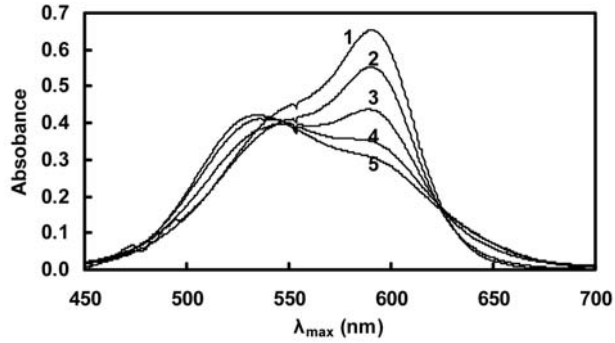

Figure 7. Absorption spectra of 6.35×10^{-6}M CV^+ in neutral solution of SDS of varying concentrations, 0 (1), 0.1 (2), 0.2 (3), 0.4 (4) and 0.5 mM SDS (5), at room temperature at the beginning of interaction.

Similar situation was reported for interaction of CV^+ with tetraphenylborate.[34] The new maximum may be attributed to formation of CV^+dimer/SDS complex. Such a behavior can be treated as an evidence of premicellar surfactant aggregation and enhanced dye dimerization by greater amount of surfactant monomers present in the solution.[35] As seen in Fig. 8, absorbance of both peaks gradually decreases.

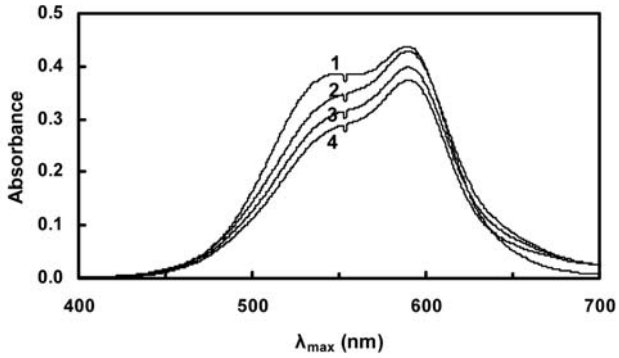

Figure 8. Absorption spectra of CV^+ in 0.2 mM SDS neutral solution at the beginning (1), 10 (2), 20 (3) and 40 minutes (4) after their interaction at 303 K.

It might have been caused due to the formation of dye-surfactant ion-pairs which progressively associate to form an aggregated type of structure.[36–38]

To measure the CV^+ fading rate constant, we prepared solution containing 6.21×10^{-6} M CV^+ and certain concentration of SDS and when equilibrium reached at 323 or 333 K, a 100 μ aliquot of 0.139 M NaOH was added into 3 ml of it. Measurements were carried out at two wavelengths, about 590 and 551.5 nm (or its shoulder) which have been interpreted on the basis of existence of two ground-state isomers of CV^+.[39–42] Results showed fading rate constants of two types of CV^+/SDS complex are similar. The *cmc* value of SDS in 0.001 N NaOH is 3.5 mM[43] and the used concentration range of SDS is below its *cmc* value, Table 6.

As seen in Table 6, the rate constant of CV^+/SDS complex fading is a function of SDS concentration. It seems that a preliminary electrostatic interaction occurs between $(CH_3)_2N^+$ = group of CV^+ molecule and negative charge on the sulfate head group of SDS and further hydrophobic interaction of SDS nonpolar moiety decreases the dielectric constant of CV^+ microenvironment. According to Hughs-Ingold rules, under these conditions, nucleophilic attack of OH^- to CV^+ is favorable. On the other hand, formation of CV^+/SDS complex reduces the positive charge of CV^+ and makes its fading reaction less favorable. Now, we study the fading reaction of CV^+ in the presence of SDS. As seen in Table 6 and Fig. 9, at 323 and 333 K, in the first region formation of CV^+/SDS complex decreases dielectric constant of CV^+ microenvironment and increases reaction rate compared to that of water. In the second region, reaction rate remains constant and in the third and fourth regions, due to increase in negative charge of CV^+/SDS complex decreases the reaction rate. As given in Table 6 (from log *K* values), formation of CV^+/SDS complex in the first region is endothermic and in the third and fourth region and thus, on the whole concentration range of SDS is exothermic.

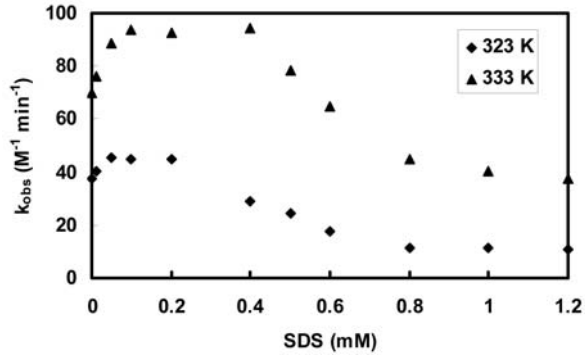

Figure 9. k_{obs} values of CV^+ fading reaction *vs.* concentrations of SDS under alkaline conditions.

3. 5. Effect of DTAB and TX-100 Mixtures on the CV^+ Fading Rate

As given in Tables 1, 4 and 7, the used concentrations of DTAB and TX-100 were in the range of their first regions at 293 K in which they have no effect on the rate of CV^+ fading separately. As seen in Table 7, an increase in DTAB or TX-100 concentration increases the reaction rate of CV^+ fading.

Table 6. Parameters Obtained from Classical model for Interaction of CV^+ with SDS at 323 and 333 K.

T (K)	Region	*sc* (mM)	k_{sc} ($M^{-1}min^{-1}$)	Samiey equation	E_s	*logK*	*n*	k_s (M^{-1} min^{-1})	Cooperativity
323	**1st**	**0.00**	**37.39**	$\ln k' = 3875.30[SDS]_t + 3.64$	–10406.8	4.84	1.01	48.18	
	2nd	0.048	45.60	**Reaction rate is approximately constant**		–	–	–	
	3rd	0.19	44.92	$\ln k' = -2379.23[SDS]_t + 4.29$	6389.2	5.52	1.57	–	
	4th	0.77	11.40	$\ln k' = -118.50[SDS]_t + 2.53$	318.2	4.53	1.72	–	
333	**1st**	**0.00**	**79.09**	$\ln k' = 4569.48[SDS]_t + 4.27$	–12650.9	5.25	1.09	93.87	
	2nd	0.097	93.98	**Reaction rate is approximately constant**		–	–	–	
	3rd	0.39	94.40	$\ln k' = -1931.84[SDS]_t + 5.29$	5348.4	4.17	1.21	–	
	4th	0.77	44.69	$\ln k' = -444.67[SDS]_t + 4.14$	1231.1	1.99	0.80	–	

Dimension of E_s is in kJ (mol molar(surfactant))$^{-1}$. Dimension of SDS concentration in Samiey equation is in M. Dimension of *K* is in M^{-n}.

Table 7. Parameters Obtained from Interaction of CV^+ with DTAB/TX-100 Mixed Micelles in the First Regions of TX-100 and DTAB at 293 K.

[DTAB] (mM)	[TX-100]	k_{obs} (M^{-1} min^{-1})	λ_{max} (nm)	Parameters
0.00	0.00	7.74 ± 0.38	589.6	K_{CVDTAB} = 66.2
0.94	1.33	16.19 ± 0.10	596.2	m = 0.73
3.09	2.13	27.05 ± 0.15	596.4	
4.85	3.08	33.76 ± 0.15	596.6	K_{CVTX} = 253.9
6.73	3.83	39.52 ± 0.18	596.8	n = 0.9
8.57	5.80	43.06 ± 0.44	597.4	

Dimensions of K_{CVDTAB} and K_{CVTX} are in M^{-m} and M^{-n}, respectively.

It is found that in the used concentrations of DTAB and TX-100, mixed micelles of them form[44–45] which results in a decrease in the apparent dielectric constant values for different mixed systems compared to those of TX-100 or DTAB solution.[46] It seems that CV^+ molecules interact with DTAB or TX-100 molecules of mixed micelles. These interactions are as follows:

$$CV^+ + nTX \leftrightarrow CVTX_n \quad K_{CVTX} = \frac{[CVTX_n]_{mic}}{[CV^+]_f [TX]^n_{mic}} \quad (7)$$

$$CV^+ + mDTAB \leftrightarrow CVDTAB_m$$
$$K_{CVDTAB} = \frac{[CVDTAB_m]_{mic}}{[CV^+]_f [DTAB]^m_{mic}} \quad (8)$$

and its reaction rate equation is as follows

$$v = k[CV^+]_t = k([CV^+]_f + [CVTX]_{mic} + [CVDTAB]_{mic}) \quad (9)$$

where k is the fading rate constant of CV^+ in water and subscripts t and f represent the total and free concentrations of CV^+, respectively. Subscript *mic* represents the concentration of surfactant in the mixed micelles. By substituting Eqs. (7) and (8) in Eq. (9) we have

$$v = k(1 + K_{CVDTAB}[DTAB]^m_{mic} + K_{CVTX}[TX]^n_{mic})[CV^+]_f = k_{obs}[CV^+]_f \quad (10)$$

where

$$k_{obs} = k(1 + K_{CVDTAB}[DTAB]^m_{mic} + K_{CVTX}[TX]^n_{mic}) \quad (11)$$

The data fitted in Eq. (11) and m, n, K_{CVDTAB} and K_{CVTX} values were given in Table 7. The results show that interaction of CV^+ with DTAB and TX-100 molecules of TX-100/DTAB mixed micelles decreases the dielectric constant of its microenvironment and thus highly increases the CV^+ fading reaction rate.

3. 6. Analysis of Kinetic Data by Cooperativity Model

The Piszkiewicz model,[47–50] analogous to the Hill model applied to the enzyme-catalyzed reactions may be considered here with some modifications. According to this model, it is assumed that substrate molecule, CV^+ in this work, associates with n number molecules of surfactant to form micelle S_nCV^+, which may react as follows:

$$nS + CV^+ \xleftrightarrow{K_D} S_nCV^+ \quad (12)$$

$$S_nCV^+ \xrightarrow{k_m} products \quad (13)$$

$$CV^+ \xrightarrow{k_w} products \quad (14)$$

The model gives the following rate equation:

$$\log[(k_{obs} - k_w)/(k_m - k_{obs})] = n\log[S]_t - \log K_D \quad (15)$$

where K_D is the dissociation constant of micellized surfactant-substrate complex back to its components and $[S]_t$ gives the total surfactant concentration. Here, k_w is the reaction rate constant without any surfactant, and k_m is the reaction rate constant with the maximum amount of surfactant concentration within the given range and if reaction is inhibited by adding surfactant, $k_m \approx 0$. n is known as the cooperativity index and is a measure of the association of additional surfactant molecules to an aggregate in the whole surfactant concentration range. If n value is greater than one, cooperativity of interaction is positive and if its value is less than one, cooperativity of interaction is negative and if its value is equal to 1, interaction is noncooperative. It is clear that Eq. (15), a two-parameter equation, can not fit properly the data of different types of surfactant-substrate interactions.

As shown in Figs. 2 and 6, there are positive catalytic effects by TX-100 and DTAB in the whole range of the reaction. As seen in Table 8, values of n show positive cooperativity in the used concentration range of DTAB and TX-100. Also, the calculated values of K_D show that binding of CV^+ to DTAB is exothermic and binding of CV^+ to TX-100 is endothermic.

Table 8. n and K_D Values Obtained from Cooperativity Model for Interaction of CV^+ with TX-100 and DTAB at 283–303 K.

T	TX-100		DTAB	
(K)	n	$\log K_D$	n	$\log K_D$
283	1.05	–1.44	18.25	–32.08
293	1.48	–1.87	14.22	–25.06
303	3.17	–4.57	12.93	–22.66

Dimension of K_D is in M^{-n}.

3. 7. Analysis of Kinetic Data by Pseudo-phase Ion Exchange (PPIE) Model

In the PPIE model, the binding constants of the interaction of surfactant molecules with CV^+ were calculated using the following equation:[51]

$$k_{obs} = \frac{k_w + k_m K_s([S]_t - cmc)}{1 + K_s([S]_t - cmc)} \quad (16)$$

where $[S]_t$, K_s, k_{obs}, k_m and k_w are the total surfactant concentration, binding constant, observed reaction rate constant and reaction rate constants in micellar media and in the bulk phase, respectively. This model can not study the surfactant-substrate interactions below the *cmc* value of surfactants. It is seen that only the data of CV^+ fading in the presence of DTAB fit in Eq. (16), Table 9.

Table 9. k_m and K_S Values Obtained from PPIE Model for Interaction of CV^+ with TX-100 and DTAB at 283–303 K.

T	TX-100		DTAB	
(K)	k_m	K_S	k_m	K_S
283	–	–	33.98	103.41
293	–	–	87.00	135.61
303	–	–	253.27	87.61

Dimensions of k_m and K_S are in M^{-1} min^{-1} and M^{-1}, respectively.

3. 8. Comparison of Substituent Effects on the CV^+, MG^+, BG^+ and $BPB^=$ Fading Rate

As seen in Table 1, fading rate constants of CV^+ in water are 2.95, 7.74 and 17.64 M^{-1} min^{-1} at 283, 293 and 303 K, respectively, whereas fading rate constants of MG^+ in water[22] are 18.89, 46.98 and 118.60 M^{-1} min^{-1} and those of BG^+ are 7.97, 20.93 and 52,05 M^{-1} min^{-1} at 283, 293 and 303 K, respectively.[20] The geometrical structure of the triphenylmethyl (trityl) system seems to be primarily responsible for the rate by which reactions takes place at the central carbon atom. Unlike CV^+ molecule, MG^+ and BG^+ have only two out of three phenyl rings substituted with dimethylamino and diethylamino groups, respectively. The two substituted rings are nearly planar aligned. The third aromatic ring is turned out of the plane of the coplanar rings. The partial planarity of MG^+ and BG^+ leaves the central carbon atom accessible for attack by the nucleophilic hydroxide ion. CV^+, on the other hand, reacts with hydroxide ion considerably slower. X-ray studies indicate that the structure of CV^+ resembles a three-bladed propeller.[23] The planes of the phenyl rings are twisted out of the plane defined by the central carbon atom and its three bonds. The twisting can be understood as a compromise between the ortho-ortho steric repulsion involving aromatic hydrogens on adjacent rings and maximum resonance stabilization of the extended conjugated π system which favors a planar conformation. Due to the propeller-shaped structure the approach of the nucleophile to the reaction center is sterically hindered and results in a drastic decrease in the fading rate constant values of CV^+ in water compared to those of MG^+ and BG^+. On the other hand, fading rate constants of $BPB^=$ in water[21] are 0.06, 0.08 and 0.263 M^{-1} min^{-1} at 298, 308 and 313 K, respectively. It seems that due to electrostatic repulsion between $BPB^=$ and OH^-, fading rate constants of $BPB^=$ is very slower than those of CV^+, MG^+, BG^+.

Binding constant values obtained from classical model for interaction of CV^+, BG^+, $BPB^=$ and MG^+ with TX-100 and DTAB at 283–303 K are shown in Table 10.[20–22] As seen in Table 10, log K_{tot} values of interaction of $BPB^=$ with TX-100 and DTAB are greater than those of CV^+, BG^+ and MG^+ which is due to the negative electric charges of $BPB^=$. As we know, positive charge of CV^+ distributes on its three aromatic rings. Also, the electron-releasing inductive effect of the ethyl groups of BG^+ is greater than that of the methyl groups of MG^+ and this makes the $(C_2H_5)_2N^+$ = group of BG^+ more stable than the $(CH_3)_2N^+$ = group of MG^+. These result in log K_{tot} values of interaction of DTAB (cationic) with these dyes change as $CV^+ > MG^+ > BG^+$ and those of interaction of TX-100 (nonionic) with these dyes change as $BG^+ > CV^+ > MG^+$.

Table 10. Comparison of log K_{tot} values obtained from classical model for interaction of CV^+, BG^+, $BPB^=$ and MG^+ with TX-100 and DTAB at 283–303 K.

T	TX-100				DTAB			
(K)	CV^+	BG^+	MG^+	$BPB^=$	CV^+	BG^+	MG^+	$BPB^=$
283	6.40	9.99	5.198	–	10.72	3.51	7.049	–
293	7.57	8.83	4.880	11.28	9.82	5.59	9.074	–
303	8.78	7.03	3.349	8.82	9.45	6.69	9.252	11.98

Dimension of K_{tot} *is in* $M^{-n_{tot}}$. BG^+ and MG^+ have two $(C_2H_5)_2N^+$ = and $(CH_3)_2N^+$ = substituent groups, respectively.

4. Conclusions

The rate constant of alkaline fading of crystal violet (CV^+) was measured in various concentrations of TX-100, DTAB and SDS. It was observed that the reaction rate constant was increased in the presence of TX-100 and DTAB. But, the fading rate increases in low concentrations of SDS and decreases in higher concentrations of SDS. The rate of fading reaction showed noticeable dependence on the electrical charge of the used surfactants. Binding constants of surfactant molecules

to CV^+ were obtained using cooperativity, pseudo-phase ion exchange and classical (or stoichiometric) models and the related thermodynamic parameters were calculated by classical (or stoichiometric) model. The results show that binding of CV^+ to TX-100 is endothermic and binding of CV^+ to DTAB and SDS is exothermic in the used concentration range of surfactants. Approach of OH^- to the reaction center in CV^+ is sterically hindered and results in a drastic decrease in the fading rate constant values of CV^+ in water compared to those of MG^+ and BG^+.

5. References

1. E. J. Fendler, J. H. Fendier, *Adv. Phys. Org. Chem.* **1970**, *8*, 271–406.
2. K. Das, B. Jain, H. S. Patel, *Spectrochim. Acta, Part A: Mol. Biomol. Spectrosc.* **2004**, *60*, 2059–2064.
3. T. Hadara, N. Nishikido, Y. Moroi, R. Matuura, *Bull. Chem. Soc. Jpn.*, **1981**, *54*, 2592– 2597.
4. H. C. Hung, T. M. Hung, G. G. Chang, *J. Chem. Soc., Perkin Trans. 2* **1997**, 2757–2760.
5. F. Merino, S. Rubio, D. Perez-Bendito, *Analyst* **2001**, *126*, 2230–2234.
6. J. H. Fendler, E. J. Fendler, *Catalysis in Micellar and Macromolecular Systems*, Academic Press, New York, **1975**.
7. S. S. Tang, G. G. Chang, *J. Org. Chem.* **1995**, *60*, 6183–6185.
8. J. Y. Liou, T. M. Huang, G. G. Chang, *J. Chem. Soc., Perkin Trans*. *2* **1999**, 2171–2176.
9. F. Jing, X. Q. An, W. G. Shen, *J. Mol. Catal. B: Enzym.* **2003**, *24–25*, 53–60.
10. R. Bermejo, D. J. Tobaruela, E. M. Talavera, A. Orte, J. M. Alvarez-Pez, *J. Colloid Interface Sci.* **2003**, *63*, 616–624.
11. D. F. Duxbury, *Chem. Rev.* **1993**, *93*, 381–433.
12. L. García-Río, J. R. Leis, J. C. Mejuto, A. Navarro-Vázquez, J. Pérez-Juste, P. Rodriguez-Dafonte, *Langmuir* **2004**, *20*, 606–613.
13. C. D. Ritchie, G. A. Skinner, V. G. Badding, *J. Am. Chem. Soc.* **1967**, *89*, 2063–2071.
14. Z. Y. Chen, J. H. Zhao, W. He, X. Q. An, W. G. Shen, *Int. J. Chem. Kinet.* **2008**, *40*, 294–300.
15. M. Y. Cheong, A. Ariffin, M. Niyaz Khan, *Bull. Korean Chem. Soc.* **2007**, *28*, 1135–1140.
16. D. G. Hall**,** *J. Phys. Chem.*, **1987**, *91*, 4287–4297.
17. J. H. Fendler, F. Nome, H. C. Van Woert, *J. Am. Chem. Soc.* **1974**, *96,* 6745–6753.
18. M. A. J. Rodgers, D. C. Foyt, Z. A. Zimek, *Radiat. Res.* **1978**, *75*, 296–304.
19. F. P. Cavasino, C. Sbriziolo, M. L. Turco Liveri, *J. Phys. Chem. B* **1998**, *102,* 5050–5054.
20. B. Samiey, M. Rafi Dargahi, *Reac. Kinet. Mech. Cat.* **2010**, *101*, 25–39.
21. B. Samiey, K. Alizadeh, M. A. Moghaddasi, M. F. Mousavi, N. Alizadeh, *Bul. Korean Chem. Soc.* **2004**, *25*, 726–736.
22. B. Samiey, A. Raoof Toosi, *Bul. Korean Chem. Soc.* **2009**, *30*, 2051–2056.
23. S. Lovell, B. J. Marquardt, B. Kahr, *J. Chem. Soc., Perkin Trans. 2* **1999**, 2241–2247.
24. Z. Huang, T. Gu, *Colloids and Surfaces* **1987**, *28*, 159–168.
25. W. Caetano, M. Tabak, *J. Colloid Interface Sci.* **2000**, *225*, 69–81.
26. R. Welti, L. J. Mulikin, T. Yoshimura, J. M. Helmkamp, *Biochemistry* **1984**, *23*, 6086–6091.
27. B. Samiey, K. Alizadeh, M. F. Mousavi, N. Alizadeh, *Bul. Korean Chem. Soc.* **2005**, *26*, 384–392.
28. S. K. Parida, B. K. Mishra, *Colloids Surf. A* **1998**, *134*, 249–255.
29. E. D. Hughes, *Trans. Faraday Soc.* **1941**, *37*, 603–631.
30. C. K. Ingold, *Structure and Mechanism in Organic Chemistry*, Bell, London, **1993**.
31. W. Linert, *Chem. Soc. Rev.* **1994**, *23*, 429– 438.
32. W. Linert, R. F. Jameson, *Chem. Soc. Rev.* **1989**, *18*, 477–505.
33. A. Chotipong, J. F. Scamehorn, T. Rirksomboon, S. Chavadej, P. Supaphol, *Colloids Surf. A* **2007**, *297*, 163–171.
34. B. G. Lee, K. S. Jung, K. J. Kim, *Bul. Korean Chem. Soc.* **1989**, *10*, 148–151.
35. M. Bielska, A. Sobczynska, K. Prochaska, *Dyes Pigments* **2009**, *80*, 201–205.
36. M. Sarkar, S. Poddar, *J. Colloid Interface Sci.* **2000**, *221*, 181–185
37. P. Pal, H. Zeng, G. Durocher, D. Girard, R. Giasson, L. Blanchard, L. Gaboury, L. Villeneuve, *J. Photochem. Photobiol. A, Chem.* **1996**, *98*, 65–72.
38. C. A. Bunton, C. H. Paik, *J. Org. Chem.* **1976**, *41*, 40–44.
39. L. García-Río, P. Hervella, J. C. Mejuto, M. Parajó, *J. Chem. Phys*. **2007**, *335*, 164–176.
40. G. N. Lewis, T. T. Magel, D. Lipkin, *J. Am. Chem. Soc.* **1942**, *64*, 1774–1782.
41. J. Korppi-Tommola, R. W. Yip, *Can. J. Chem.* **1981**, *59*, 191–195.
42. Y. Maruyama, M. Ishikawa, H. Satozono, *J. Am. Chem. Soc.* **1996**, *118*, 6257–6263.
43. M. Rabiller-Baudry, L. Paugam, L. Bégion, D. Delaunay, M. Fernandez-Cruz, C. Phina-Ziebin, C. Laviades-Garcia de Guadiana, B. Chaufer, *Desalination* **2006**, *191*, 334–343.
44. M. S. Mandeep, S. Shweta, K. Singh, A. Shaheen, *J. Colloid Interface Sci.* **2005**, *286*, 369–377.
45. O. A. Soboleva, G. A. Badun, B. D. Summ, *Colloid Journal* **2006**, *68*, 255–263.
46. C. Carnero Ruiz, J. Aguiar, *Langmuir* **2000**, *16*, 7946–7953.
47. D. J. Piszkiewicz, *J. Am. Chem. Soc.* **1976**, *98*, 3053–3055.
48. D. J. Piszkiewicz, *J. Am. Chem. Soc.* **1977**, *99*, 7695–7697.
49. D. J. Piszkiewicz, *J. Am. Chem. Soc.* **1977**, *99*, 1550–1557.
50. http://en.wikipedia.org/wiki/Hill_equation
51. M. Mahta, L. B. T. Sundari, K. C. Raiana, *Int. J. Chem. Kinet.* **1996**, *28*, 637–648.

Povzetek

V temperaturnem območju med 283 in 303 K samo proučevali hitrost alkalnega razbarvanja barvila kristal vijolično (CV^+) v prisotnosti neionskega (TX-100), kationskega (DTAB) in anionskega (SDS) surfaktanta. Ugotovili smo, da je konstanta reakcijske hitrosti razbarvanja večja v prisotnosti TX-100 in DTAB ter manjša v pristnosti SDS. Določili smo tudi konstante vezanja med CV^+ in TX-100 ter DTAB in SDS ter po stehiometričnem modelu izračunali ustrezne termodinamske parametre. Rezultati kažejo, da je v obravnavanem koncentracisjkem območju surfaktantov vezava CV^+ in TX-100 endotermni proces, medtem ko je vezava med CV^+ in DTAB kot tudi SDS eksotermna.

Supporting information

Table S1. Hughs–Ingold Rules for Solvent Effects in Nucleophilic Substitution Reactions.

Reaction	Reactants	Transition state	Change in charge distribution	Effect of increasing solvent polarity	Size of effect
S_N2	$Y^- + R–X$	$^{\delta-}Y \ldots R \ldots X^{\delta-}$	Dispersed	Decrease	Small
S_N2	$Y + R–X$	$^{\delta+}Y \ldots R \ldots X^{\delta-}$	Increased	Increase	Large
S_N2	$Y^- + R–X^+$	$^{\delta-}Y \ldots R \ldots X^{\delta+}$	Decreased	Decrease	Large
S_N2	$Y + R–X^+$	$^{\delta+}Y \ldots R \ldots X^{\delta+}$	Dispersed	Decrease	Small
S_N1	R–X	$^{\delta+}R \ldots \ldots X^{\delta-}$	Increased	Increase	Large
S_N1	$R–X^+$	$^{\delta+}R \ldots \ldots X^{\delta+}$	Dispersed	Decrease	Small

The electrophilic-nucleophilic combination reaction occurs in the reverse direction of S_N1 reaction of R–X.

Table S2. Equations of $\Delta S^{\neq}$ ($J\ mol^{-1}\ K^{-1}$) versus $\Delta H^{\neq}$ ($kJ\ mol^{-1}$) Values of CV^+

Fading Reaction in the Presence of TX-100.		
First region	$\Delta S^{\neq} = 3.337\ \Delta H^{\neq} - 223.54$	$R^2 = 0.999$
Second region	$\Delta S^{\neq} = 2.992\ \Delta H^{\neq} - 203.68$	$R^2 = 0.981$
Third region	$\Delta S^{\neq} = 4.092\ \Delta H^{\neq} - 251.92$	$R^2 = 0.978$

Table S3. Equations of $\Delta S^{\neq}$ ($J\ mol^{-1}\ K^{-1}$) versus $\Delta H^{\neq}$ ($kJ\ mol^{-1}$) Values of CV^+

Fading Reaction in the Presence of DTAB.		
First region	$\Delta S^{\neq} = 3.945\ \Delta H^{\neq} - 260.86$	$R^2 = 0.998$
Second region	$\Delta S^{\neq} = 2.267\ \Delta H^{\neq} - 142.77$	$R^2 = 0.999$
Third region	$\Delta S^{\neq} = 3.716\ \Delta H^{\neq} - 232.50$	$R^2 = 0.999$

k_{obs} values for interaction of MG^+ with TX-100, DTAB and SDS at 283–303 K (from ref. 22) for comparison with those of BG^+ are given as follows:

Table S4. k_{obs} values for interaction of MG^+ with TX-100 at 283–303 K.

$[TX]_t$ (mM)	k_{obs} ($M^{-1}\ min^{-1}$) at 283 K	293 K	303 K
0.00	18.89	46.98	118.60
0.113	23.04	51.32	129.697
0.583	33.10	66.99	148.677
1.136	38.57	72.615	161.73
3.335	46.97	85.88	189.00
4.86	50.14	97.04	206.53
7.222	59.16	115.40	235.00
8.928	65.08	125.80	250.54
10.002	70.17	132.498	264.00
20.013	82.985	158.23	281.80
29.952	86.47	162.45	285.92
49.984	89.81	167.36	287.24
60.101	90.98	169.25	288.25

Table S5. k_{obs} values for interaction of MG^+ with DTAB at 283–303 K.

$[DTAB]_t$ (mM)	k_{obs} ($M^{-1}\ min^{-1}$) at 283 K	293 K	303 K
0.00	18.89	46.98	118.60
2.774	19.60	47.82	119.26
5.954	20.01	49.61	120.50
10.69	21.01	51.52	121.94
14.74	21.84	53.60	123.20
18.59	31.97	71.47	171.02
21.82	52.45	112.55	249.67
26.25	74.22	169.65	349.54
29.62	110.49	247.03	487.03
35.14	116.35	260.89	530.85
40.12	125.24	270.12	569.21

Table S6. k_{obs} values for interaction of MG^+ with SDS at 283–303 K.

$[SDS]_t$ (mM)	k_{obs} ($M^{-1}\ min^{-1}$) at 283 K	293 K	303 K
0.00	18.89	46.98	118.60
0.298	17.80	45.31	115.01
0.718	16.46	42.22	108.11
1.019	15.45	39.94	102.89
1.31	12.23	28.14	86.235
1.54	9.62	21.63	75.99
2.129	8.33	19.59	67.58
2.982	5.70	16.14	50.45
4.917	3.41	10.32	32.09
6.914	2.75	8.16	25.05
10.18	2.28	6.74	18.59
12.02	2.09	6.01	15.02